Palaeogeography, Palaeoclimatology, Palaeoecology 496 (2018) 175–182

Contents lists available at ScienceDirect

Palaeogeography, Palaeoclimatology, Palaeoecology

journal homepage: www.elsevier.com/locate/palaeo

Evolution of integrated lake status since the last deglaciation: A high-resolution sedimentary record from Lake Gonghai, Shanxi, China

Shengqian Chen[a], Jianbao Liu[a,*], Chengling Xie[a], Jianhui Chen[a], Haipeng Wang[a], Zongli Wang[a], Zhiguo Rao[a], Qinghai Xu[b], Fahu Chen[a]

[a] Key Laboratory of West China's Environmental System (Ministry of Education), Lanzhou University, Lanzhou 730000, China
[b] Institute of Nihewan Archaeology Research, College of Resources and Environment, Hebei Normal University, Shijiazhuang 050024, China

ARTICLE INFO

Keywords:
Alpine lake
Climate change
East Asian summer monsoon
Local humidity

ABSTRACT

Alpine lakes not only provide internationally important habitats for endangered species, they also play a crucial role in the regional water balance. Unfortunately, a rapid loss of alpine lakes in China has occurred in recent decades; however, intensive human activities, together with regional differences in the responses of lakes to climate change, has impeded our understanding of the contribution of climate change to the loss of these lakes. To better understand how alpine lakes will evolve with continuing global warming, we used the analysis of new sedimentary proxies from Lake Gonghai, an undisturbed alpine lake, together with a review of published records, to reconstruct variations in integrated lake status since the last deglaciation. From 14,660–11,890 cal. yr BP the lake was in the most unstable state, indicated by the highest amplitude fluctuations in lake level and the within-lake environment. The lake status experienced clear millennial-scale changes. During the early and middle Holocene (11,890–3200 cal. yr BP), the most stable lake status occurred, consistent with the highest precipitation levels. Owing to the highest level of freshwater influx in the middle Holocene (8–5 ka), the lake water was the deepest and most acidic. At this time, the dense vegetation cover resulted in maximum catchment stability and the lowest level of soil erosion, and hence the lowest sediment accumulation rate. From 3200 cal. yr BP, decreasing mean annual precipitation resulted in a moderately stable lake status, a shallow water depth and more alkaline lake water. The sparse vegetation cover caused a dramatic increase in the erosion rate and hence in the sediment accumulation rate. We infer that variations in local humidity were the major control on the integrated lake status during the last ~14,600 cal. yr BP. With the anticipated progression of global warming, the status of the alpine lakes in the region may continue to deteriorate and appropriate mitigation strategies are imperative.

1. Introduction

Lakes are a major component of the global ecosystem, representing a total fresh water storage of 175,000 km^3 (Oki and Kanae, 2006). Furthermore, they provide internationally important wetland habitats for endangered animals and migratory birds (e.g. McLaughlin and Cohen, 2013). Because of their remote location, alpine lakes are relatively uninfluenced by human activities; thus, they are regarded as sensitive monitors of global climate change (Adrian et al., 2009) and have played an important role in reconstructing past climate variability. In addition, lake sediments contain a broad spectrum of physical, geochemical and biological indicators and provide continuous, high resolution records of changes in terrestrial and aquatic ecosystems (e.g. Kröpelin et al., 2008). However, previous studies of alpine lakes have focused mainly on the history and mechanisms of climate change, and few studies have been made of the integrated response of both lakes and their catchments to climate change, especially in arid and semi-arid regions.

Global climate change may fundamentally alter the integrated lake status (Eastwood et al., 1999; Ye et al., 2013; Liu et al., 2017a). For example, recent anthropogenic climate change has significantly changed the status of many lakes. In China, the number and size of lakes with a surface area greater than 1 km^2 has decreased significantly during the past half-century, because of both climate change and intensive human activities (Ma et al., 2010). Specifically, a rapid loss of alpine lakes in the last few decades has been reported on the Mongolian Plateau (Tao et al., 2015) and in Xinjiang Province (Ma et al., 2010). However, in contrast, the number and size of lakes on the Tibetan Plateau has increased significantly (Ma et al., 2010; Zhang et al., 2017), which suggests that some alpine lakes are exhibiting the opposite

* Corresponding author at: Key Laboratory of West China's Environmental System (Ministry of Education), Lanzhou University, 222 South Tianshui Road, Lanzhou 730000, China.
E-mail address: jbl@lzu.edu.cn (J. Liu).

https://doi.org/10.1016/j.palaeo.2018.01.035
Received 28 November 2017; Received in revised form 22 January 2018; Accepted 22 January 2018
Available online 01 February 2018
0031-0182/

response to recent global warming compared to lakes elsewhere. Unfortunately, human activities make it difficult to isolate the contribution of climate change to the evolution of alpine lakes, and therefore systematic studies of their response to past climate change are becoming increasingly important.

The Chinese Loess Plateau (CLP) is one of the earliest and most important hearths of Chinese Neolithic cultures, such as the Dadiwan Culture (8.2–7.4 ka) and the Laoguantai Culture (8–7 ka) (Hosner et al., 2016) and has long been recognized as the cradle of Chinese civilization. The current human population of the CLP is over 100 million. A small group of alpine lakes is located on the northeastern margin of the CLP and they play an important role in the regional water balance; however, within the last ten years the number of these lakes has decreased from 11 to 3 (Wang et al., 2014a). The reasons for their rapid demise and the response of the existing lakes to continued global warming is unclear. Reconstructing the impact of natural climate change on the integrated lake status in this region may improve our understanding of the causes of the recent rapid loss of alpine lakes in China as a whole.

Lake Gonghai is a hydrologically-closed alpine lake on the CLP and its well-dated sediment record and undisturbed catchment make it an ideal site to study the effects of climate change on integrated lake status. Recently, proxies such as pollen assemblages (Chen et al., 2015), magnetic susceptibility (MS; Chen et al., 2013) and chemical index of alteration (CIA; Liu et al., 2017b) from Lake Gonghai were used to reconstruct the evolution of regional moisture. However, there were mismatches between the different proxies and the indicative significance of new proxies (e.g., grain-size distributions) have not been well explained. In the present study, we present the results of the analysis of new proxies from the sediments of Lake Gonghai and focus on their interpretation. Then, we consider the problems intrinsic to several of the proxies. Finally, we combine the new data and published records to reconstruct the variations in integrated lake status since the last deglaciation.

2. Study area

2.1. Physical setting

Lake Gonghai (38°54′N, 112°14′E; 1860 m above sea level) is formed on a planation surface between the Sanggan and Fenhe river drainages. It is located in Ningwu county, Shanxi Province, north China (Fig. 1A), near the modern summer monsoon limit and in the farming-pastoral ecotone of north China. Previously, there were 11 alpine lakes on the planation surface but currently only 3 remain.

Lake Gonghai (Fig. 1B) is hydrologically-closed and the main water source is from precipitation and ground water. There are no inlets or outlets. It has a surface area of ~0.36 km^2, a maximum water depth of ~10 m and a flat lake bed. The mean annual precipitation of the area is 468 mm, with more than 77% occurring between June and September. We infer from the lake beach ridges that lake water has not outflowed since the lake was formed. The regional bedrock consists mainly of reddish sandstone of Mesozoic age (Wang et al., 2014a). The regional vegetation is dominated by *Larix principis-rupprechtii*, *Pinus tabulaeformis* and *Populus davidiana* forest, while *Hippophae rhamnoides* scrub, *Bothriochloa ischaemum* grassland and *Carex* spp. are widely distributed within the catchment (Chen et al., 2015). Based on historical documents, intensive deforestation did not occur until ~600 cal. yr BP (Zhang et al., 2007) and therefore Lake Gonghai is well suited for a study of the response of lake status to climate change because of the limited influence of human activity since the last deglaciation.

2.2. Sources of the lake sediments

Based on stratigraphic and structural evidence, Lake Gonghai was formed around 16 ka by tectonic activity (Wang et al., 2014a). Based on our observations, the lake sediments can be divided into three components in terms of their origin: from surface runoff produced by intensive rainfall which entrains particulate material and transports it to the lake, with coarse grains deposited near the lakeshore and fine-grained sediments carried to the center; background dust and dust storm deposition; and ice-trapped dust (Fig. 2).

3. Materials and methods

3.1. Lithology and chronology

Core GH09B has a length of 9.8 m. The interval from 9.80–9.42 m consists mainly of sand and gravel. The upper 9.42 m is composed of lake sediments which can be divided into three lithological units (Fig. 3), as follows: Unit 3 (9.42–7.70 m) consists of alternating layers of light-dark silt and dark, silty clay with the occasional occurrence of yellow sand; Unit 2 (7.70–2.60 m) consists of dark organic mud with light grey mud between 4.70 and 2.60 m; and Unit 1 (2.60–0.00 m) consists of silty clay with occasional plant macrofossils. Core GH09C is a parallel core to GH09B, with a length of 9.3 m. Comparison of the sedimentary facies and MS records of the two cores indicates a high degree of similarity (Fig. 3D and E).

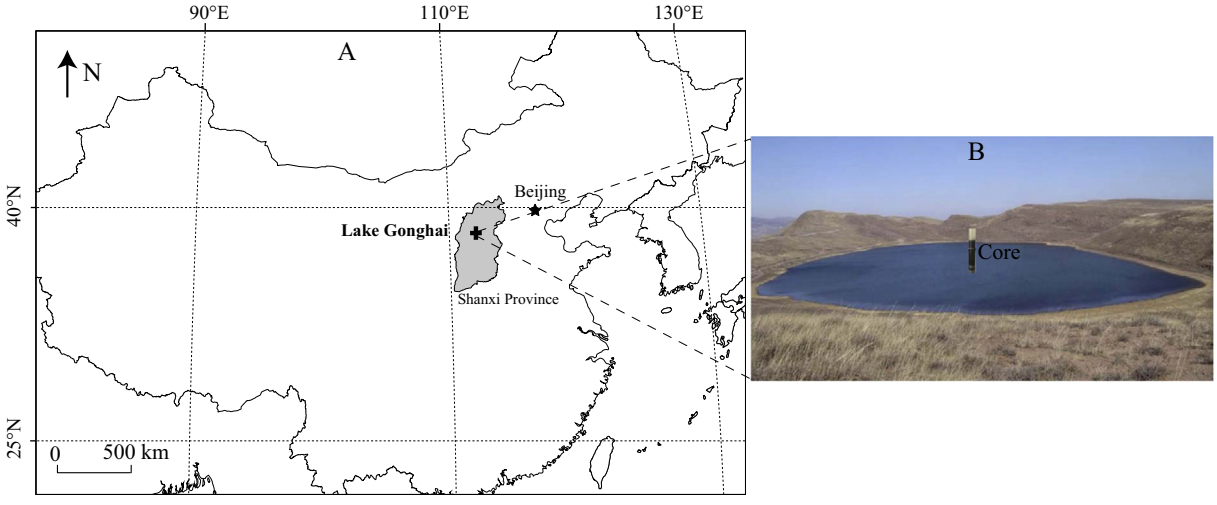

Fig. 1. Physical setting of Lake Gonghai. A, location of Lake Gonghai in Shanxi Province in central north China. B, panorama of Lake Gonghai and its catchment in Lvliang Mountain, and location of the sediment cores (Wan et al., 2016).

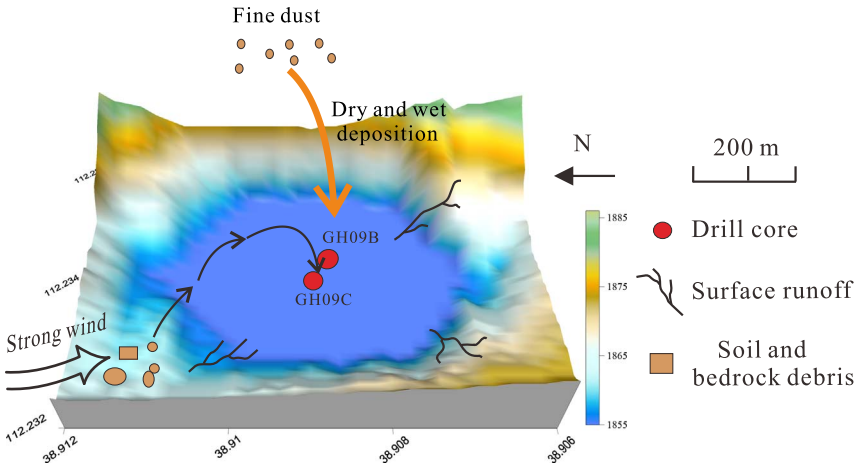

Fig. 2. Schematic diagram of the sources of mineral sediment in Lake Gonghai. The yellow arrow indicates dry and wet deposition of fine dust in high altitude. The black arrows represent dust storm deposition via surface wind. (For interpretation of the references to colour in this figure legend, the reader is referred to the web version of this article.)

The upper 35 cm of GH09B was dated by a combination of ^{210}Pb and ^{137}Cs. In addition, a total of 25 terrestrial plant macrofossil samples (18 from core GH09B and 7 from core GB09C) were selected for AMS ^{14}C dating at Beta Analytic Inc. and the Xi'an AMS Laboratory. The ^{14}C sample depths for core GH09C were transferred to corresponding depths in GH09B based on high resolution correlation of the MS and lithology records of the two cores (Fig. 3D and E). The conventional radiocarbon ages were calibrated to calendar years using the IntCal09 calibration curve (Reimer et al., 2009), and Bayesian age-depth modeling was performed using OxCal v4.2.2 and a Poisson-process (P-sequence) single depositional model at a 1-cm increment with a K value of 100 (Ramsey, 2008). The radiocarbon ages of GH09B and GH09C are illustrated in Fig. 3 (Chen et al., 2015). The average sediment accumulation rates of the three units of GH09B are 62 cm/kyr (Unit 3), 42 cm/kyr (Unit 2) and 239 cm/kyr (Unit 1).

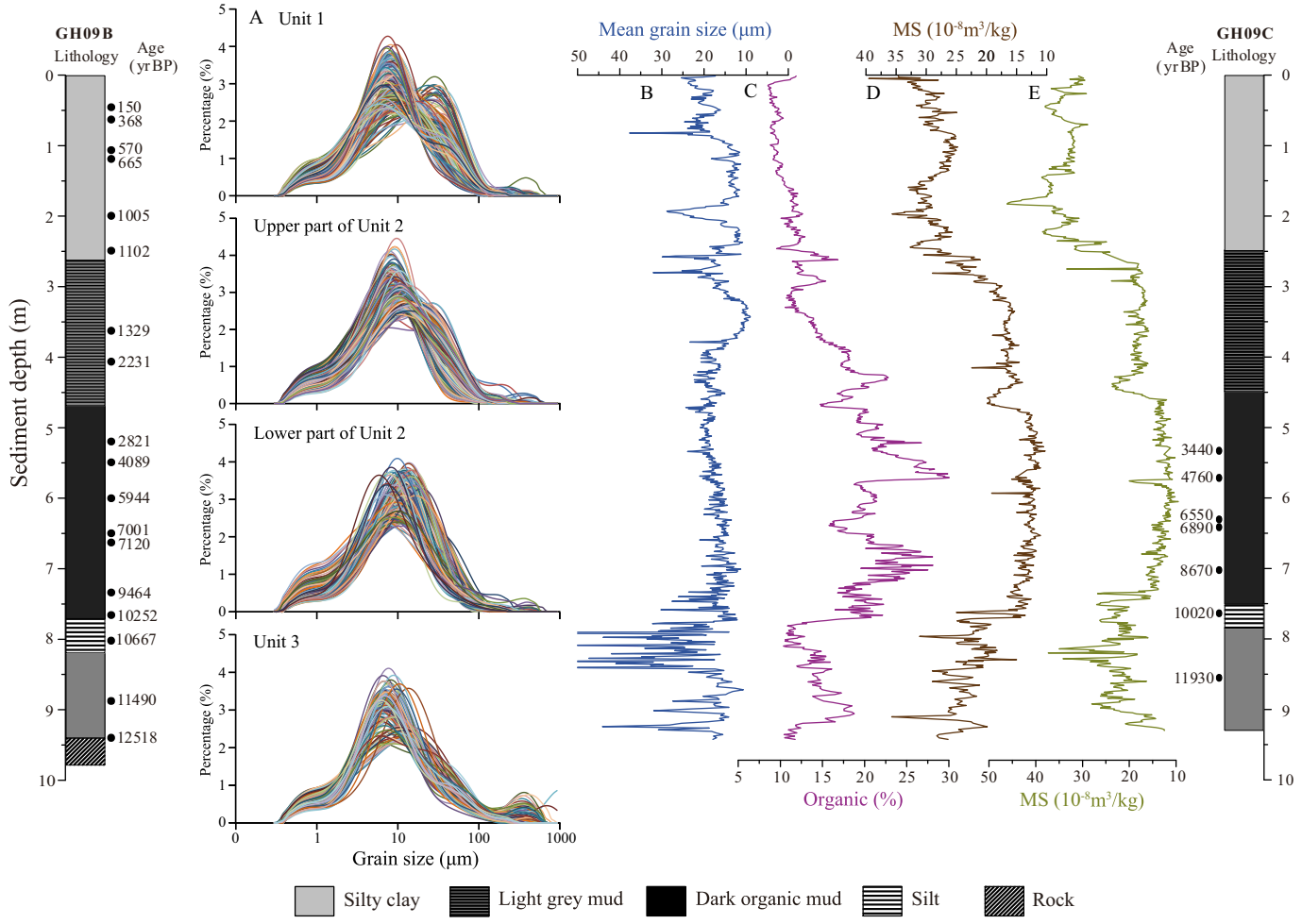

Fig. 3. Lithology and location of AMS ^{14}C dates for core GH09B and core GH09C, and comparison of proxy records. A, grain-size distributions of samples from GH09B. B, mean grain-size of core GH09B. C, organic carbon content of core GH09B. D, magnetic susceptibility record for core GH09B. E, magnetic susceptibility record of core GH09C.

3.2. Laboratory methods

Core GH09B was sampled at a ~1-cm interval, yielding 774 samples with an average time resolution of 20 yr. Grain-size analysis was conducted using a Malvern Mastersizer 2000 following standard pretreatment procedures: 1) 0.2 g of lake sediments were heated with 10 ml of 30% H_2O_2 to remove organic matter; 2) 10 ml of 10% HCl were added to remove carbonate; 3) 150 ml of distilled water were added to remove acidic ions; 4) after leaving for 24 h, the particles were dispersed by adding 10 ml 0.5 N $(NaPO_3)_6$ and by ultrasonic (Lu and An, 1997). Organic matter content (OMC) was measured using the loss-on-ignition (LOI) method (Heiri et al., 2001).

The sixty-one samples from core GH09C were selected for measurement of carbon-to-nitrogen (C/N) molar ratios using a Vario EL elemental analyzer. The following pretreatment procedure was used: 1) 10 ml of 10% HCl were added to 0.5 g lake sediments to remove carbonate; 2) distilled water was repeatedly added to the residues to render the solution neutral; 3) the samples were oven-dried at 40 °C.

4. Results

The variations in mean grain-size coincide with variations in lithology (Fig. 3B). The mean grain-size is relatively high and exhibits high amplitude and rapid fluctuations in Unit 3 and Unit 1, but the values are significantly lower and generally very stable in Unit 2. The lowest and most stable values occur in the lower part of Unit 2. Representative grain-size distributions of samples from Unit 1 are clearly trimodal (Fig. 3A); the three components are clay, fine silt and coarse silt. In contrast, the grain-size distribution curve of samples from Unit 2 are bimodal, especially in the lower part of Unit 2. The two components are clay and fine silt; the coarse silt component only occurs in a few samples in the upper part of Unit 2 (Fig. 3A). The grain-size distribution curves of samples in the lower part of Unit 2 are very similar. In Unit 3, the grain-size distributions have four components (Fig. 3A); in addition, to the three components mentioned above, a sand component is present, which explains the occurrence of the highest mean grain-size in this unit.

The C/N molar ratios were highest during the last deglaciation, and exhibit a decreasing trend during the transition between the last deglaciation and the Holocene. The values were stable during the early and middle Holocene, and gradually decreased since ~4 ka (Fig. 4A). The OMC was relatively low during cold intervals, such as the Younger Dryas (YD); however, it increased sharply during the Bølling/Allerød (B/A) and the early Holocene. The OMC decreased abruptly during 8–6 ka, and commenced a decreasing trend during the middle-to-late Holocene (Fig. 3C).

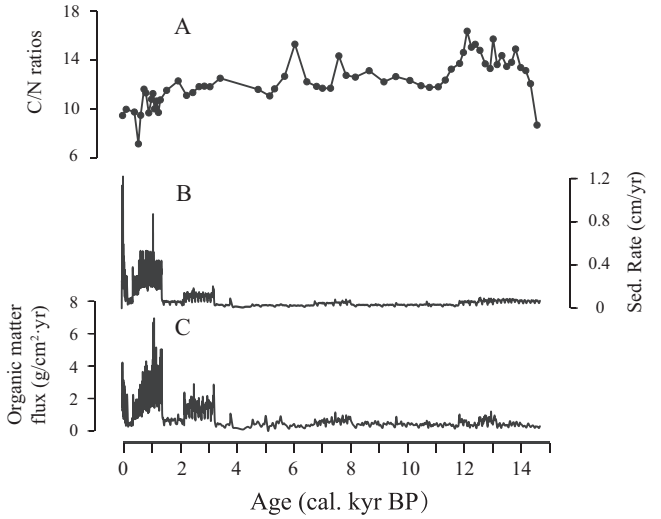

Fig. 4. A, time series of C/N ratios; B, sediment accumulation rate; C, MARoc of organic matter. The sediment accumulation rate and MARoc were calculated by every two samples.

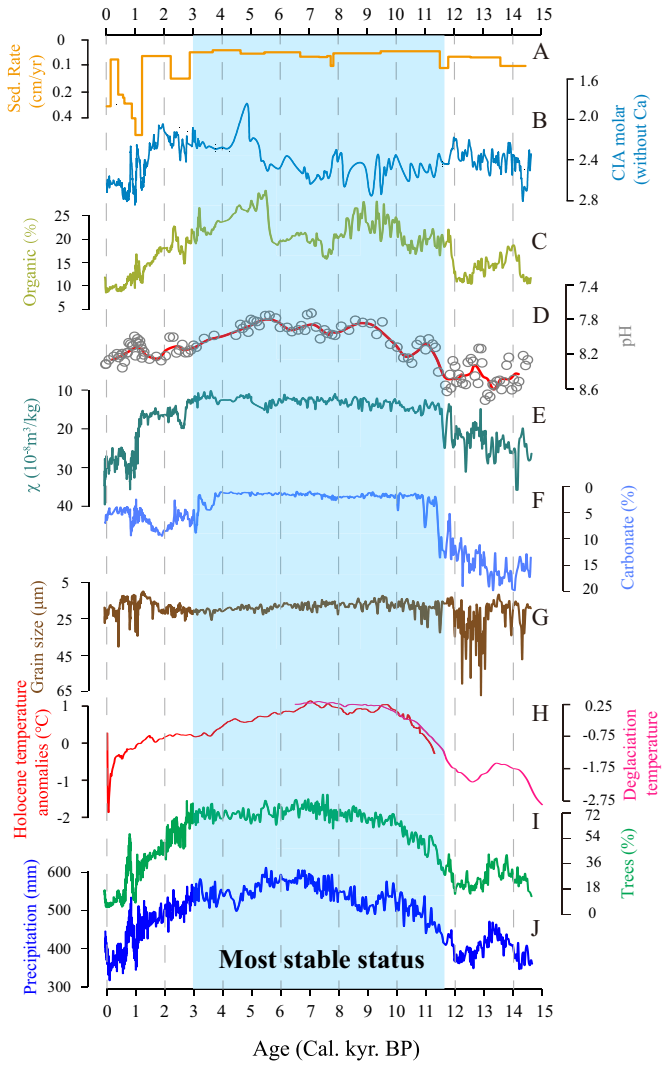

Fig. 5. Time series of various environmental proxies for Lake Gonghai and regional climate records. A, sediment accumulation rate calculated by every two radiocarbon ages. B, CIA molar ratio, excluding Ca (Liu et al., 2017b). C, organic matter content. D, lake water pH (Cao et al., 2017). E, magnetic susceptibility (Chen et al., 2013). F, carbonate content. G, mean grain-size. H, Northern hemisphere temperature during the last deglaciation (pink curve; Shakun et al., 2012) and the Holocene (red curve; Marcott et al., 2013). I, percentage of tree pollen. J, pollen-based annual precipitation reconstruction for Lake Gonghai (Chen et al., 2015). (For interpretation of the references to colour in this figure legend, the reader is referred to the web version of this article.)

5. Discussion

5.1. The anomalous change in organic matter content during 8–6 ka

The organic matter content of lake sediments mainly reflects lake productivity (An et al., 2011) and the input of terrestrial organic material. The main source of organic matter in lake sediments is particulate plant detritus, which can be divided into an exogenetic fraction and an authigenic fraction (Meyers and Lallier-Vergès, 1999). The origin of the organic matter can be determined by the C/N ratios. For example, phytoplankton typically has C/N ratios of 4–10, whereas vascular land plants have C/N ratios of 20 or higher (Meyers and Ishiwatari, 1993).

The pattern of variation of the OMC of the Gonghai lake sediments resembles that of pollen-inferred precipitation; however, the OMC

decreased abruptly when the annual precipitation was highest (Fig. 5C and J), which conflicts with the previous view (e.g. Xiao et al., 2006). During the interval of OMC decrease, the pollen assemblages reveal a maximum in the frequencies of broad-leaved trees (Chen et al., 2015; Xu et al., 2016). Similarly, the $\delta^{13}C$ of long-chain *n*-alkanes indicates that during 8–5 ka the vegetation within the Gonghai catchment was overwhelmingly dominated by C_3 plants, which further supports the pollen record (Rao et al., 2016). Moreover, a regional mid-Holocene monsoonal rainfall maximum is also supported by a synthesis of paleosol development based on 310 dates from 77 sites on the CLP (Wang et al., 2014b), paleosol occurrence based on 335 dates from 75 sites in the dunefields of eastern China (Li et al., 2014), and by the pollen record from Daihai Lake (Xiao et al., 2004). Therefore, we infer that the decrease in sedimentary OMC at Lake Gonghai during the mid-Holocene does not reflect a decrease in the strength of the East Asian summer monsoon (EASM).

To remove the influence of other sedimentary components on the OMC record, we calculated the mass accumulation rate (MAR_{oc}) of organic carbon, as follows:

$$MAR_{oc}(g\ cm^{-2}\ yr^{-1}) = LSR \times DBD \times f \quad (1)$$

where LSR is the linear sediment accumulation rate (cm/yr, calculated from every two samples), DBD is the sediment dry bulk density (g/cm^3), and f is the fraction of organic matter. Because the bulk sediment accumulation rate during the late Holocene was very much higher than previously (by a factor of up to 240), the variation of MAR_{oc} closely tracks the changes in bulk sediment accumulation rate (Fig. 4B and C), and thus is also in disagreement with the pattern of evolution of monsoonal rainfall.

The C/N molar ratios of the Lake Gonghai sediments range from 9.5–15.3, with the highest value during the last deglaciation and the lowest value during the late Holocene (Fig. 4A). The average C/N ratio between 8 and 6 ka was ~13, indicating a roughly equal mixture of algal and vascular land plant material (Meyers and Lallier-Vergès, 1999). The forest cover was highest during 8–6 ka, as indicated by pollen assemblages and the $\delta^{13}C$ of *n*- alkanes (Chen et al., 2015; Rao et al., 2016). In addition, the bulk sediment accumulation rate during this interval was the lowest (Fig. 5A) and the grain size was the finest (Fig. 5G). Thus, we conclude that the lowest level of soil erosion occurred during this interval, with the loss of mineral material and terrestrial organic matter from the catchment being minimized by the densest vegetation cover. At the same time, the high lake level and relatively deep water reduced light penetration which was unfavorable for the growth of algae. In addition, there was no change in the pollen percentages of aquatic vegetation during this interval (Xu et al., 2016). Therefore, we conclude that the anomalous change in sedimentary OMC during the mid-Holocene was mainly the result of the very low level of soil erosion rather than a decrease in monsoonal rainfall. In addition, this result also demonstrates that sediment accumulation rate had little effect on the organic matter content. Consequently, we conclude that caution is needed in the use of the OMC of lake sediments as an indicator of paleorainfall.

5.2. The evolution of integrated lake status since the last deglaciation

The evolution of integrated lake status can be characterized by two aspects: changes in the within-lake environment and changes in the lake catchment. In this section, we use new sedimentary proxies from Lake Gonghai, together with a review of published proxies, to reconstruct the evolution of the integrated lake status.

5.2.1. The last deglaciation (9.42–7.70 m, 14,660–11,890 cal. yr BP)

During this period, the temperature of the Northern Hemisphere (Shakun et al., 2012) and annual rainfall in north China (Chen et al., 2015) exhibited a distinct pattern of millennial-scale variations. For example, following the warm and wet B/A interstadial, a significant decrease in temperature and annual rainfall occurred during the YD cold period (Fig. 5H and J). At Lake Gonghai, the sedimentary indicators all exhibit unstable behavior with the largest fluctuations during the entire study interval. Based on a comparison of the MS values of lake sediments and catchment bedrock, a high sediment accumulation rate (~65 cm/kyr), and the presence of sand from weathered bedrock, Chen et al. (2013) argued that bedrock erosion, soil erosion and wind-blown dust all contributed to the supply of detrital magnetic minerals during this interval. In addition, the multiple components evident in the grain-size distributions reflect different transportation or depositional processes (Sun et al., 2002), emphasizing that the source of the sediments was complex. Chemical weathering within the lake catchment was weak during this stage, as indicated by the low CIA molar ratios (Fig. 5bB; Liu et al., 2017b). Moreover, the lower humidity of the local climate (Fig. 5D) resulted in increased carbonate precipitation (Fig. 5F) since the catchment lacks carbonate minerals, as well as the relatively high lake water pH (ranging from 8.17–8.73; Cao et al., 2017). The occurrence of high amplitude fluctuations in MS and carbonate content indicate unstable within-lake and catchment environments. The changes in the proxies enable the development of the catchment and lake status to be divided into two sub-stages:

5.2.1.1. Sub-stage 1A (9.42–8.42 m, 14,660–13,100 cal. yr BP). This sub-stage commenced with the formation of the Lake Gonghai basin (Wang et al., 2014a). Its age is consistent with the B/A warming interval as indicated by the Greenland NGRIP ice core (North Greenland Ice Core Project members, 2004). Together with an increase in temperature and precipitation during the interstadial, the percentage of tree pollen and OMC increased significantly (Fig. 5C and I). Nevertheless, the local vegetation remained dominated by shrubs and herbs such as *Artemisia*, Chenopodiaceae, and Gramineae. In response to the increase in forest cover (from 12 to 40%), the sedimentary grain-size decreased sharply and the lake sediments were mainly composed of mineral grains derived from lake catchment erosion and eolian dust.

In addition, the chironomid assemblage of the Lake Gonghai sediments was dominated by *Nanocladius*, *Corynoneura edwardsi*-type and *Psectrocla-dius sordidellus*-type, indicating a shallow lake and a temperate environment (Wang et al., 2016). In summary, the lake was in an early stage of development under a mild and less arid climate.

5.2.1.2. Sub-stage 1B (8.42–7.70 m, 13,100–11,890 cal. yr BP). Within the uncertainties of the chronology, this sub-stage corresponds to the YD cold event. The temperature, precipitation and forest cover decreased significantly (Fig. 5I and J), and the local vegetation was dominated by herbs such as *Artemisia* and Chenopodiaceae. The inferred vegetation changes are supported by the $\delta^{13}C$ values of long-chain *n*-alkanes. The negative $\delta^{13}C$ values indicate that the local vegetation was dominated by C_3 grasses, because the cold climate would have inhibited the growth of C_4 plants (Rao et al., 2016).

The sharp reduction in sedimentary OMC indicates that primary productivity was low (An et al., 2011; Fig. 5C). The sedimentary mean grain-size increased dramatically, reaching a maximum, and it also fluctuated significantly (Fig. 5G), mainly due to the small lake surface area. The chironomid assemblages also indicate that the lake was still shallow (Wang et al., 2016). The rapid changes in environment significantly affected the lake status; for example, *Chironomus anthracinus*-type and *C. plumosus*-type are present in the sediments, which are often the result of significant environmental change (Brooks, 1997; Wang et al., 2016).

5.2.2. Early and middle Holocene (7.70–5.20 m, 11,890–3200 cal. yr BP)

Following the increase in summer insolation of the Northern Hemisphere (Laskar et al., 2004), temperature and annual precipitation in north China increased significantly during the transition from the late glacial to the Holocene (Fig. 5H and J). The temperature was highest during the early and middle Holocene and was followed by a

significant decrease after 7 ka (Marcott et al., 2013). At Lake Gonghai, deciduous trees such as *Quercus* and *Betula* dominated the local vegetation; broad-leaved tree pollen frequencies reached their maximum abundance during 7.8–5.3 ka (Xu et al., 2016), which is consistent with the $\delta^{13}C$ values of *n*-alkanes (Rao et al., 2016). Using the weighted averaging partial least squares model, Chen et al. (2015) and Liu et al. (2015, 2017c) proposed that the highest precipitation in north China occurred in the mid-Holocene; however, this is inconsistent with the prevailing view of an early Holocene EASM maximum mainly inferred from Chinese speleothem $\delta^{18}O$ records (Dykoski et al., 2005).

The integrated lake status responded immediately to the changing climate. During this interval, the forest cover was denser than either before or after, as indicated by the proportion of tree pollen in the lake sediments (Fig. 5I). The relatively dense forest cover resulted in the lowest catchment erosion rate and thus the sediment accumulation rate was the lowest (~30 cm/kyr). Chen et al. (2013) proposed that the supply of magnetic minerals from the catchment was minimal. The consistent bimodal grain-size distribution also indicates that the depositional processes of the lake sediments were similar (Fig. 3A). Furthermore, Liu et al. (2017b) argued that while physical erosion was weak, the high CIA molar ratios and the highest percentage of fine-grained sediments indicate the occurrence of strong chemical weathering (Fig. 5B). As noted previously, the weak physical erosion but strong chemical weathering led to a decrease in sedimentary OMC during the mid-Holocene.

With regard to the within-lake environment, the sedimentary MS values, carbonate content and grain size were relatively uniform during this interval (Fig. 5E, F and G). Although the OMC decreased sharply during this interval, the trends of all the indicators indicate an integrated lake status of maximum stability and the highest lake level. In detail, the abundant input of freshwater resulted in the lake water becoming unsaturated with respect to carbonate and hence the carbonate content of the lake sediments decreased sharply and then remained stable. Although rainfall was increasing, the MS values decreased significantly because of the high degree of vegetation cover and resulting soil stability within the catchment (Chen et al., 2013). This inference is supported by the occurrence of the lowest sediment accumulation rates. The decrease in sediment grain-size may have resulted from a combination of two factors. First, the East Asian winter monsoon (EAWM) weakened significantly during the transition from late glacial to Holocene, as indicated by the sea surface temperature gradient in the southern South China Sea (Huang et al., 2011), changes in a magnetic susceptibility record from Huguang Maar Lake (Yancheva et al., 2007) and in a grain-size index in the Okinawa Trough (Zheng et al., 2014); thus the grain-size of the wind-blown dust was finer. Second, the size of Lake Gonghai may have been larger because of the higher precipitation, and the sediments in the lake center delivered by surface runoff would be expected to be finer-grained, given that the grain size of lake sediments gradually decreases from the shore to the center (Xiao et al., 2012). A lake level maximum during this interval is also supported by the chironomid assemblages (Wang et al., 2016) and by the lowest lake water pH (Cao et al., 2017).

5.2.3. Late Holocene (5.20–0 m, 3200 cal. yr BP - present)

Temperature and precipitation decreased continuously during this interval, except during the Medieval Warm Period when precipitation increased sharply (Fig. 5H and J). The proportion of tree pollen decreased from 70% to 5%, and that of herb pollen increased from 25% to 90%. The herbs were mainly dominated by *Artemisia* and Chenopodiaceae (Xu et al., 2016). The $\delta^{13}C$ values of *n*-alkanes were ~ − 30‰, suggesting a mixture of C_3 and C_4 vegetation (Rao et al., 2016).

The sediment accumulation rate (~163 cm/kyr) was much higher than previously (Fig. 5A). The grain-size distributions in this interval (Unit 1 and the upper part of Unit 2) are clearly trimodal, which indicates a new source of lake sediments compared to the early and middle Holocene. In fact, a thin loess layer (designated L0) was formed on the CLP during this interval, overlying the Holocene soil (S0) (An et al., 1993). However, the accumulation rate of loess on the CLP (which reached a maximum of ~20 cm/kyr during glacial intervals) (Chen et al., 1991), and the maximum MS values of eolian dust, were much lower than those of the Lake Gonghai sediments. Hence, although dust storm deposition contributed to the observed very high sediment accumulation rates at Lake Gonghai and can explain the trimodal distribution of lake sediments, it was proportionally insignificant. We suggest that soil erosion was responsible for the high accumulation rate, since the degree of catchment instability was lower, and vegetation cover was sparse due to the weakening of the EASM. This interpretation is supported by a comparison of the MS values of lake sediments and catchment soil (Chen et al., 2013), and by the CIA molar ratios (Fig. 5B; Liu et al., 2017b). Moreover, the abnormal increase in the sediment accumulation rate may also due to human activity. Numerous pollen grains of crop plants were identified at 1300 cal. yr BP (Xu et al., 2016), which is consistent with the highest accumulation rate (Fig. 5A).

Because of the decreased annual precipitation, the sedimentary OMC decreased continuously, from 21% to 9% (Fig. 5C), reflecting a decrease in the primary productivity of the lake ecosystem. In addition, the lake water pH was higher than during the early and mid-Holocene (Fig. 5D). This change is consistent with the variation of the carbonate content, which increased from 2% to 7% (Fig. 5F). There was also a renewed increase in the grain size of the lake sediments (Fig. 5G). The relatively large fluctuations in carbonate content and grain size indicate that the lake system was unstable. At the same time, the contribution of deep-water taxa to the chironomid assemblages decreased abruptly in response to the decrease in precipitation, while that of the shallow water taxa increased sharply and they came to dominate the assemblages (Wang et al., 2016).

The coldest temperatures occurred during the Little Ice Age (Marcott et al., 2013), coincident with the weakest EASM of the entire Holocene (Chen et al., 2015). This extreme weak EASM event, together with the YD event, resulted in a lower buffering capacity of the within-lake environment and lake catchment, as indicated by pronounced variations in all indicators. By contrast, during other arid events, although annual precipitation decreased (e.g., during the 8.2 ka event), it still remained at a high level. As a result, the within-lake environment and lake catchment had a higher buffering capacity, due to the higher precipitation and forest cover, enabling it to accommodate arid and cold events and thus some of the indicators did not record these events. Therefore, we suggest that precipitation/humidity was responsible for driving the evolution of the integrated lake status.

Continuing global warming is expected to result in a drier climate in the arid and semi-arid region of China (Held and Soden, 2006; Huang et al., 2017), which is likely to accelerate the rate of loss of alpine lakes. In addition, human activities such as the exploitation of mineral and groundwater resources will further damage lake ecosystems. Although the Chinese government has implemented a series of environmental protection policies, more effective actions are imperative to protect these alpine lakes in the future.

6. Conclusions

To better understand how alpine lakes responded to climate change, we used records of grain size and organic matter content, together with a review of published records from well-dated sediment cores, to reconstruct the evolution of the integrated status of Lake Gonghai and its catchment since the last deglaciation. Both the within-lake environment and the surrounding catchment responded rapidly to climate change, which fundamentally changed their stability in terms of vegetation cover, erosion rate and lake water chemistry.

During the last deglaciation (14,660–11,890 cal. yr BP), the relatively low precipitation and temperature resulted in the most unstable integrated lake status, including a sparse forest cover, moderate erosion rate, shallow lake level and higher lake water pH. The early

development stage of the integrated lake status during the Bølling-Allerød interstadial was interrupted by the Younger Dryas cold interval, during which the various proxies exhibited the highest amplitude fluctuations. During the early and middle Holocene (11,890–3200 cal. yr BP), the occurrence of maximum rainfall was consistent with the most stable integrated lake status. During the mid-Holocene, the densest forest cover led to the lowest soil erosion and sediment accumulation rates, which resulted in a decrease in the organic matter content of the lake sediments. Because of the strong influx of freshwater, pH values were the lowest during this interval, consistent with the lowest carbonate content and the maximum lake water depth as indicated by the chironomid assemblages. Since 3200 cal. yr BP, a moderately unstable integrated lake status is indicated by rapid changes in magnetic susceptibility values and in carbonate content. The cool and dry climate reduced the vegetation cover of the catchment, resulting in the most intense soil erosion and highest sediment accumulation rate. The pH values increased again due to the decrease in freshwater influx.

Overall, our results indicate that the integrated lake status was closely related to the local humidity. In addition, the results shed light on the processes by which alpine lakes and their catchments respond to climate change. With continuing global warming, the expected drier climate in arid and semi-arid regions will accelerate the degeneration of the alpine lakes, and they are also susceptible to damage by intensive human activities. Therefore, more effective actions are imperative for protecting these valuable lake ecosystems.

Acknowledgments

We sincerely thank Prof. J.W. Zhang who gave helpful suggestions; S.J. Gao and Dr. Q. Li who participated in the laboratory analyses. The work was jointly supported by the National Natural Science Foundation of China (41790421, 41471162, 41601186, 41130102) and Fundamental Research Funds for the Central Universities (Grant lzujbky-2016-271, lzujbky-2016-279).

References

Adrian, R., O'Reilly, C.M., Zagarese, H., Baines, S.B., Hessen, D.O., Keller, W., Livingstone, D.M., Sommaruga, R., Straile, D., Van Donk, E., Weyhenmeyer, G.A., Winder, M., 2009. Lakes as sentinels of climate change. Limnol. Oceanogr. 54, 2283–2297.

An, Z.S., Porter, S.C., Zhou, W.J., Lu, Y.C., Donahue, D.J., Head, M.J., Wu, X.H., Ren, J.Z., Zheng, H.B., 1993. Episode of strengthened summer monsoon climate of Younger Dryas age on the Loess Plateau of central China. Quat. Res. 39, 45–54.

An, Z.S., Clemens, S.C., Shen, J., Qiang, X.K., Jin, Z.D., Sun, Y.B., Prell, W.L., Luo, J.J., Wang, S.M., Xu, H., Cai, Y.J., Zhou, W.J., Liu, X.D., Liu, W.G., Shi, Z.G., Yan, L.B., Xiao, X.Y., Chang, H., Wu, F., Ai, L., Liu, F.Y., 2011. Glacial-interglacial Indian summer monsoon dynamics. Science 333, 719–723.

Brooks, S.J., 1997. The response of Chironomidae (Insecta: Diptera) assemblages to late-glacial climatic change in Kråkenes Lake, western Norway. Quaternary Proceedings 5, 49–58.

Cao, J.T., Rao, Z.G., Ji, G.D., Xu, Q.H., Chen, F.H., 2017. A 15 ka pH record from an alpine lake in north China derived from the cyclization ratio index of aquatic brGDGTs and its paleoclimatic significance. Org. Geochem. 109, 31–46.

Chen, F.H., Li, J.J., Zhang, W.X., 1991. Loess stratigraphy of the Lanzhou profile and its comparison with deep-sea sediment and ice core record. GeoJournal 24 (2), 201–209.

Chen, F.H., Liu, J.B., Xu, Q.H., Li, Y.C., Chen, J.H., Wei, H.T., Liu, Q.S., Wang, Z.L., Cao, X.Y., Zhang, S.R., 2013. Environmental magnetic studies of sediment cores from Lake Gonghai: implications for monsoon evolution in North China during the late glacial and Holocene. J. Paleolimnol. 49, 447–464.

Chen, F.H., Xu, Q.H., Chen, J.H., Birks, H.J., Liu, J.B., Zhang, S.R., Jin, L.Y., An, C.B., Telford, R.J., Cao, X.Y., Wang, Z.L., Zhang, X., Selvaraj, K., Lu, H.Y., Li, Y.C., Zheng, Z., Wang, H.P., Zhou, A.F., Dong, G.H., Zhang, J.W., Huang, X.Z., Bloemendal, J., Rao, Z.G., 2015. East Asian summer monsoon precipitation variability since the last deglaciation. Sci. Rep. 5, 11186.

Dykoski, C.A., Edwards, R.L., Cheng, H., Yuan, D.X., Cai, Y.J., Zhang, M.L., Lin, Y.S., Qing, J.M., An, Z.S., Revenaugh, J., 2005. A high-resolution, absolute-dated Holocene and deglacial Asian monsoon record from Dongge Cave, China. Earth Planet. Sci. Lett. 233, 71–86.

Eastwood, W.J., Roberts, N., Lamb, H.F., Tibby, J.C., 1999. Holocene environmental change in southwest Turkey: a palaeoecological record of lake and catchment-related changes. Quat. Sci. Rev. 18, 671–695.

Heiri, O., Lotter, A.F., Lemcke, G., 2001. Loss on ignition as a method for estimating organic and carbonate content in sediments: reproducibility and comparability of results. J. Paleolimnol. 25 (1), 101–110.

Held, I.M., Soden, B.J., 2006. Robust responses of the hydrological cycle to global warming. J. Clim. 19, 5686–5699.

Hosner, D., Wagner, M., Tarasov, P.E., Chen, X.C., Leipe, C., 2016. Spatiotemporal distribution patterns of archaeological sites in China during the Neolithic and Bronze Age: an overview. The Holocene 26, 1576–1593.

Huang, E.Q., Tian, J., Steinke, S., 2011. Millennial-scale dynamics of the winter cold tongue in the southern South China Sea over the past 26 ka and the East Asian winter monsoon. Quat. Res. 75, 196–204.

Huang, J.P., Yu, H.P., Dai, A.G., Wei, Y., Kang, L.T., 2017. Drylands face potential threat under 2 °C global warming target. Nat. Clim. Chang. 6, 166–171.

Kröpelin, S., Verschuren, D., Lézine, A.M., Eggermont, H., Cocquyt, C., Francus, P., Cazet, J.P., Fagot, M., Rumes, B., Russel, J.M., Darius, F., Conley, D.J., Schuster, M., von Suchodoletz, H., Engstrom, D.R., 2008. Climate-driven ecosystem succession in the Sahara: the past 6000 years. Science 320, 765–768.

Laskar, J., Robutel, P., Joutel, F., Gastineau, M., Correia, A.C.M., Levrard, B., 2004. A long-term numerical solution for the insolation quantities of the earth. Astron. Astrophys. 428, 261–285.

Li, Q., Wu, H.B., Yu, Y.Y., Sun, A.Z., Marković, S.B., Guo, Z.T., 2014. Reconstructed moisture evolution of the deserts in northern China since the Last Glacial Maximum and its implications for the East Asian Summer Monsoon. Glob. Planet. Chang. 121, 101–112.

Liu, J.B., Chen, J.H., Zhang, X.J., Li, Y., Rao, Z.G., Chen, F.H., 2015. Holocene East Asian summer monsoon records in northern China and their inconsistency with Chinese stalagmite $\delta^{18}O$ records. Earth Sci. Rev. 148, 194–208.

Liu, J.B., Rühland, K.M., Chen, J.H., Xu, Y.Y., Chen, S.Q., Chen, Q.M., Huang, W., Xu, Q.H., Chen, F.H., Smol, J.P., 2017a. Aerosol-weakened summer monsoons decrease lake fertilization on the Chinese Loess Plateau. Nat. Clim. Chang. 7, 190–194.

Liu, J.B., Chen, J.H., Kandasamy, S., Chen, S.Q., Xie, C.L., Chen, Q.M., Lin, B.Z., Yu, K.F., Xu, Q.H., Velasco, V.M., Chen, F.H., 2017b. A 14.7 ka record of earth's surface processes from the arid-monsoon transitional China. Earth Surf. Process. Landf. http://dx.doi.org/10.1002/esp.4265.

Liu, J.B., Chen, S.Q., Chen, J.H., Zhang, Z.P., Chen, F.H., 2017c. Chinese cave $\delta^{18}O$ records do not represent northern East Asian summer monsoon rainfall. Proc. Natl. Acad. Sci. 114, E2987–2988.

Lu, H.Y., An, Z.S., 1997. Pretreated methods on loess-palaeosol samples granulometry. Chin. Sci. Bull. 43, 237–240.

Ma, R.H., Duan, H.G., Hu, C.M., Feng, X.Z., Li, A.N., Ju, W.M., Jiang, J.H., Yang, G.S., 2010. A half-century of changes in China's lakes: global warming or human influence? Geophys. Res. Lett. 37, L24106. http://dx.doi.org/10.1029/2010GL045514.

Marcott, S.A., Shakun, J.D., Clark, P.U., Mix, A.C., 2013. A reconstruction of regional and global temperature for the past 11,300 years. Science 339, 1198–1201.

McLaughlin, D.L., Cohen, M.J., 2013. Realizing ecosystem services: wetland hydrologic function along a gradient of ecosystem condition. Ecol. Appl. 23, 1619–1631.

Meyers, P.A., Ishiwatari, R., 1993. Lacustrine organic geochemistry—an overview of indicators of organic matter sources and diagenesis in lake sediments. Org. Geochem. 20, 867–900.

Meyers, P.A., Lallier-Vergès, E., 1999. Lacustrine sedimentary organic matter records of Late Quaternary paleoclimates. J. Paleolimnol. 21, 345–372.

North Greenland Ice Core Project members, 2004. High-resolution record of Northern Hemisphere climate extending into the last interglacial period. Nature 431, 147–151.

Oki, T., Kanae, S., 2006. Global hydrological cycles and world water resources. Science 313, 1068–1072.

Ramsey, C.B., 2008. Deposition models for chronological records. Quat. Sci. Rev. 27, 42–60.

Rao, Z.G., Jia, G.D., Li, Y.X., Chen, J.H., Xu, Q.H., Chen, F.H., 2016. Asynchronous evolution of the isotopic composition and amount of precipitation in north China during the Holocene revealed by a record of compound-specific carbon and hydrogen isotopes of long-chain n-alkanes from an alpine lake. Earth Planet. Sci. Lett. 446, 68–76.

Reimer, P.J., Baillie, M.G., Bard, E., Bayliss, A., Beck, J.W., Blackwell, P.G., Ramsey, C.B., Buck, C.E., Burr, G.S., Edwards, R.L., Friedrich, M., Grootes, P.M., Guilderson, T.P., Hajdas, I., Heaton, T.J., Hogg, A.G., Hughen, K.A., Kaiser, K.F., Kromer, B., McCormac, F.G., Manning, S.W., Reimer, R.W., Richards, D.A., Southon, J.R., Talamo, S., Turney, C.S.M., van der Plicht, J., Weyhenmeyer, C.E., 2009. IntCal09 and Marine09 radiocarbon age calibration curves, 0–50,000 years cal BP. Radiocarbon 51, 1111–1150.

Shakun, J.D., Clark, P.U., He, F., Marcott, S.A., Mix, A.C., Liu, Z., Otto-Bliesner, B., Schmittner, A., Bard, E., 2012. Global warming preceded by increasing carbon dioxide concentrations during the last deglaciation. Nature 484, 49–54.

Sun, D.H., Bloemendal, J., Rea, D.K., Vandenberghe, J., Jiang, F.C., An, Z.S., Su, R.X., 2002. Grain-size distribution function of polymodal sediments in hydraulic and aeolian environments, and numerical partitioning of the sedimentary components. Sediment. Geol. 152, 263–277.

Tao, S.L., Fang, J.Y., Zhao, X., Zhao, S.Q., Shen, H.H., Hu, H.F., Tang, Z.Y., Wang, Z.H., Guo, Q.H., 2015. Rapid loss of lakes on the Mongolian Plateau. Proc. Natl. Acad. Sci. 112, 2281–2286.

Wan, D.J., Song, L., Yang, J.S., Jin, Z.D., Zhan, C.J., Mao, X., Liu, D.W., Shao, Y., 2016. Increasing heavy metals in the background atmosphere of central North China since the 1980s: evidence from a 200-year lake sediment record. Atmos. Environ. 138, 183–190.

Wang, X., Wang, Z.L., Chen, J.H., Liu, J.B., Wang, H.P., Zhang, S.R., Chen, F.H., 2014a. On the origin of the upland lake group in Ningwu Tianchi region, Shanxi Province. Journal of Lanzhou University (Natural Sciences) 50, 208–212.

Wang, H.P., Chen, J.H., Zhang, X.J., Chen, F.H., 2014b. Palaeosol development in the Chinese Loess Plateau as an indicator of the strength of the East Asian summer monsoon: evidence for a mid-Holocene maximum. Quat. Int. 334, 155–164.

Wang, H.P., Brooks, S.J., Chen, J.H., Hu, Y., Wang, Z.L., Liu, J.B., Xu, Q.H., Chen, F.H., 2016. Response of chironomid assemblages to East Asian summer monsoon precipitation variability in northern China since the last deglaciation. J. Quat. Sci. 31, 967–982.

Xiao, J.L., Xu, Q.H., Nakamura, T., Yang, X.Y., Liang, W.H., Inouchi, Y., 2004. Holocene vegetation variation in the Daihai Lake region of north-central China: a direct indication of the Asian monsoon climatic history. Quat. Sci. Rev. 23, 1669–1679.

Xiao, J.L., Wu, J.T., Si, B., Liang, W.D., Nakamura, T., Liu, B.L., Inouchi, Y., 2006. Holocene climate changes in the monsoon/arid transition reflected by carbon concentration in Daihai Lake of Inner Mongolia. The Holocene 16, 551–560.

Xiao, J.L., Chang, Z.G., Fan, J.W., Zhou, L., Zhai, D.Y., Wen, R.L., Qin, X.G., 2012. The link between grain-size components and depositional processes in a modern clastic lake. Sedimentology 59, 1050–1062.

Xu, Q.H., Chen, F.H., Zhang, S.R., Cao, X.Y., Li, J.Y., Li, Y.C., Li, M.Y., Chen, J.H., Liu, J.B., Wang, Z.L., 2016. Vegetation succession and East Asian Summer Monsoon changes since the last deglaciation inferred from high-resolution pollen record in Lake Gonghai, Shanxi Province, China. The Holocene 27, 835–846.

Yancheva, G., Nowaczyk, N.R., Mingram, J., Dulski, P., Schettler, G., Negendank, J.F., Liu, J.Q., Sigman, D.M., Peterson, L.C., Haug, G.H., 2007. Influence of the intertropical convergence zone on the East Asian monsoon. Nature 445, 74–77.

Ye, X.C., Zhang, Q., Liu, J., Li, X.H., Xu, C.Y., 2013. Distinguishing the relative impacts of climate change and human activities on variation of streamflow in the Poyang Lake catchment, China. J. Hydrol. 494, 83–95.

Zhang, H.Z., Wang, S.Y., Cao, Z.M., 2007. Discussion on the historical stage division of basin ecological safety——taking Fenhe River upstream as the subjects. Journal of Taiyuan Normal University 6, 1–5.

Zhang, G.Q., Yao, T.D., Piao, S.L., Bolch, T., Xie, H.J., Chen, D.L., Gao, Y.H., O'Reilly, C.M., Shum, C.K., Yang, K., Yi, S., Lei, Y.B., Wang, W.C., He, Y., Shang, K., Yang, X.K., Zhang, H.B., 2017. Extensive and drastically different alpine lake changes on Asia's high plateaus during the past four decades. Geophys. Res. Lett. 44, 252–260.

Zheng, X.F., Li, A.C., Wan, S.M., Jiang, F.Q., Kao, S.J., Johnson, C., 2014. ITCZ and ENSO pacing on East Asian winter monsoon variation during the Holocene: Sedimentological evidence from the Okinawa Trough. Journal of Geophysical Research: Oceans 119, 4410–4429.